Flexural behavior of ambient cured reinforced geopolymer concrete beams

[1]Geetha K, [2]S Vijaya, [3]Akash C M
[1]Associate professor,[2]Professor and HOD,[3]M.Tech student
[1]Department of Civil Engineering,
[1]East West Institute of Technology, [2]Dr.Ambedkar Institute of Technology,[3]Dr.Ambedkar Institute of Technology, Bengaluru, India

Abstract - Glass-fiber reinforced polymer (GFRP) bars embedded in geopolymer concrete (GPC) can provide strong, long-lasting structures. The flexural behavior of reinforced GPC beams is examined in the present work. There are totally two types of beams with same reinforcement ratio, GPC beams reinforced with steel bars and GPC beams reinforced with GFRP bars. Each beam was tested by four-point loading. GPC beams are cured at ambient temperature. Studies were conducted on ultimate load and ultimate mid-span deflection behavior. The ultimate load carrying capacity was found by increasing trend by using GFRP bars. GFRP bars reduces the ultimate mid-span deflection. The experimental findings for each beam were validated by a Finite element analysis (FEA) using ANSYS 2022. The experimental and analytical results were showing the same trend and the results are varying between 11.9-15.3%.

Index Terms - Flexural behavior, Geopolymer concrete (GPC), Glass fiber reinforced polymer (GFRP) bars, Finite element analysis (FEA).

I. INTRODUCTION

The engineering and construction sectors have paid substantial attention to geopolymer, an innovative and ecologically friendly substance. In contrast to conventional cement-based materials, geopolymer is created by a chemical reaction between an aluminosilicate source and an alkaline activator, producing a long-lasting and high-strength substance. In comparison to OPC, GPC emits 64% less carbon dioxide during the course of manufacture. Geopolymer Concrete (GPC) and Ordinary Portland Cement (OPC), are two distinct materials, and each have unique characteristics and production processes. Environmental concerns are exacerbated by the fact that cement produces significant carbon dioxide emissions. While GPC uses industrial waste that has been alkaline solution activated or silica and alumina-rich natural resources, it is a more environmentally responsible choice. GPC is often employed at higher temperatures, so using nano-silica, an attempt is made to cure GPC beams at ambient temperature. GPC have an advantages of Reduced carbon footprint, Greater strength and durability, water conservation and improved workability, utilization of industrial by-products and fire resistance. Nano silica has made a significant breakthrough in the field of civil engineering by enhancing the performance of cement and concrete-based composites and ushering in a new age of design for construction materials. which has particle sizes ranging from 1 to 100 nanometers. The properties of nano silica are Improved mechanical properties, enhanced durability, cost, greater flexural and compressive strength and reduced cracking and shrinkage. In structural engineering and construction, two materials that are often utilized are steel and fiber-reinforced polymer (FRP). Fibers and resin matrix are the two distinct phases that make up Fiber Reinforced Polymer (FRP) composite materials. Steel is a conventional material that has been widely used in many applications because of its strong strength and durability. Steel is nonetheless prone to corrosion, particularly in harsh settings, which need routine maintenance and might raise lifespan costs. FRP composites are made of high-strength fibers, such carbon or glass inserted in a polymer matrix. FRP is ideal for a variety of applications, notably in maritime and corrosive conditions because to its outstanding strength-to-weight ratio and corrosion resistance. It is simpler to transport and construct FRP structures since they frequently weigh less than steel and don't need anti-corrosion coatings. FRP may also be customized to meet unique needs and has great fatigue resistance.

II. LITERATURE SURVEY

Chunhua Lu et al (2022), In this work, using a combination of steel bars and glass-fiber reinforced polymer (GFRP), the flexural behaviour of steel-fiber-reinforced concrete (SC) beams is examined. evaluating experimental findings for the new SC beams in comparison to earlier studies on plain concrete (PC) beams. Stirrups in this case make use of 8mm-diameter steel bars. The test results, including cracking load, failure mechanism, ultimate load, crack spacing and breadth, and mid-span deflection, are thoroughly studied for seven tested SC beams with varying nominal reinforcement ratios and designs. The flexural behaviour of PC and SC beams with equivalent reinforcements are carefully compared in the study. The study also looks at how test beams' failure mechanisms are strongly impacted by the type of concrete and flexural strength. as some or all of the steel bars are replaced with GFRP bars, the cracking load is reduced but the ultimate load is higher as compared to five steel-fiber-reinforced concrete (SC) beams with the same total area of steel and GFRP bars. According to this, the hybrid-reinforced SC beams have a better load-carrying capability but less fracture resistance than the steel-reinforced SC beams.

O. H. Zinkaah et al (2022), In this study, the flexural performance of geopolymer concrete (FRP-GPC) beams reinforced using polymer bars is evaluated using theoretical and numerical techniques. The ABAQUS programme was used to generate nonlinear finite-element models using experimental data from the literature. Numerous factors were the subject of parametric analyses, including compressive strength, the kind of FRP reinforcement, the shear reinforcement ratio, and the shear span-to-depth (a/h) ratio. The results showed the same trend between FE results and experimental data for failure mechanism, failure load, and load-deflection response. When beams are not reinforced with webs, compressive strength had a considerable impact on load capacity. Low a/h ratios and a lack of web reinforcement made compressive strength the controlling factor in shear behaviour. It was demonstrated that shear reinforcement levels up to 0.7% on the web were sufficient to prevent shear failure and had no impact on load capacity.

III. METHODOLOGY

Geopolymer concrete (GPC) with a nano-silica base was used in this experiment. The GPC mix contained Commercial grade-Class-F fine and coarse aggregate. The work uses fly ash, nano silica, 12M sodium hydroxide (NaoH), and sodium silicate (Na2Sio3). The mix design for the M25 grade for GPC is provided in [Table 1]. [Table 2] provides a summary of the properties of GPC over a period of 28 days, including compressive strength (f_c) of size 150x150x150mm, split tensile strength (f_t) of size 150x300mm, young's modulus (E) of size 150x300mm, and flexural strength (f_f) of size 500x100x100mm. Bars made of both steel and GFRP are used in the investigation. E-glass that has been impregnated with vinyl ester resin is used to make GFRP bars. The steel and GFRP bars used have nominal diameters of 10 and 12 mm and 8 mm diameter stirrups, respectively. Information about the GFRP bars' characteristics was provided by the manufacturer.

Table 1. Mix design of GPC.

Mix proportion for GPC						
Particular	**Fly ash**	**Nano silica**	**FA**	**CA**	**NaoH**	**Na_2Sio_3**
Kg/m^3	468.18	11.92	628.193	1166.65	65.158	162.895

Table 2. Properties of GPC.

Concrete type	**f_c**	**f_t**	**E**	**f_f**
GPC (N/mm^2)	33.72	3.61	19523.8	5.12

1. Experimental Investigation

The beams measuring 1200mm in length, 300mm in depth, and 230mm in breadth. GPC beam reinforced with Steel bars and GPC beam reinforced with GFRP bars are studied with reinforcement ratio of 0.83% which is under reinforced section and details are shown in [Table 3].

Table 3. Tested beam details.

Specimen	Type of concrete	Type of reinforcement bar	Top bar dia (mm)	Bottom bar dia (mm)	Reinforcement Section	Reinforcement Ratio (%)
Geo_ns-1	GPC	Steel	2#10	3#12	Under reinforced	0.83
Geo_ns-2	GPC	GFRP	2#10	3#12	Under reinforced	0.83

1.1. Test setup

The beams were put through a four-point static bending test until they broke after 28 days of curing. It makes use of a loading frame with a 30T capacity. A hydraulic jack is used to place a load on the beam. To evenly distribute weight over the rollers that are fastened to the beam, the hydraulic jack is positioned above the beam. The rollers are positioned above the test beam at two points where the load must be applied. 50mm bearing is taken into account on both sides of the beam. Each of the three segments of 1100mm measures 275mm, 550mm, and 275mm. The loading point is 550mm apart from each load and 275mm from the beam on either side. Three linear variable displacement transducers, or LVDTs, were used to gauge the specimen's deflection. The specimen's midspan is where one LVDT is located, and the other two are on either side of the beam. The test set was built as shown in [Figure 1] in order to conduct it.

Figure 1. Test setup for beams.

1.2. Analytical Validation

The models are created in ANSYS 2022, a finite element analysis (FEA), using the same dimensions and properties as the actual data to examine the flexural performance of the beam. The beam models were developed using the same configuration as in the experimental work and are described in [Table 3]. As shown in [Figure 2], a static load is applied to the beam model. Results from the model's static load analysis are gathered.

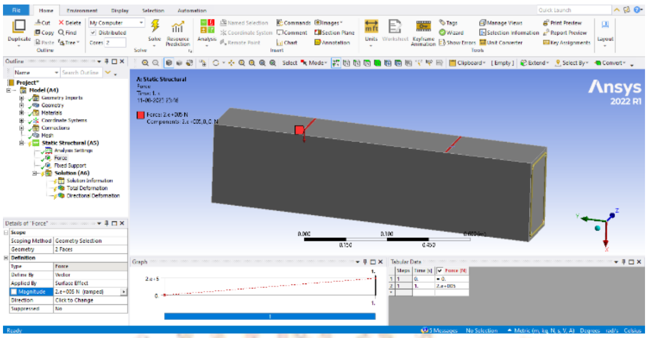

Figure 2. Model of beam in Ansys.

IV. Results and Discussion

1. Experimental results

1.1. Ultimate load

The ultimate load-carrying capacity of GPC beams are illustrated in [Figure 3]. It can be identified that, Geo_ns-2 beam have ultimate load of 79kN whereas Geo_ns-1 beam have ultimate load of 62kN. Geo_ns-2 beam have more ultimate load carrying capacity with respect to Geo_ns-1. It is found that, the GPC beams with GFRP bars have more ultimate load than GPC beams with steel bars. That is, GFRP bars has more tensile strength than steel bars, so the ultimate load is increased.

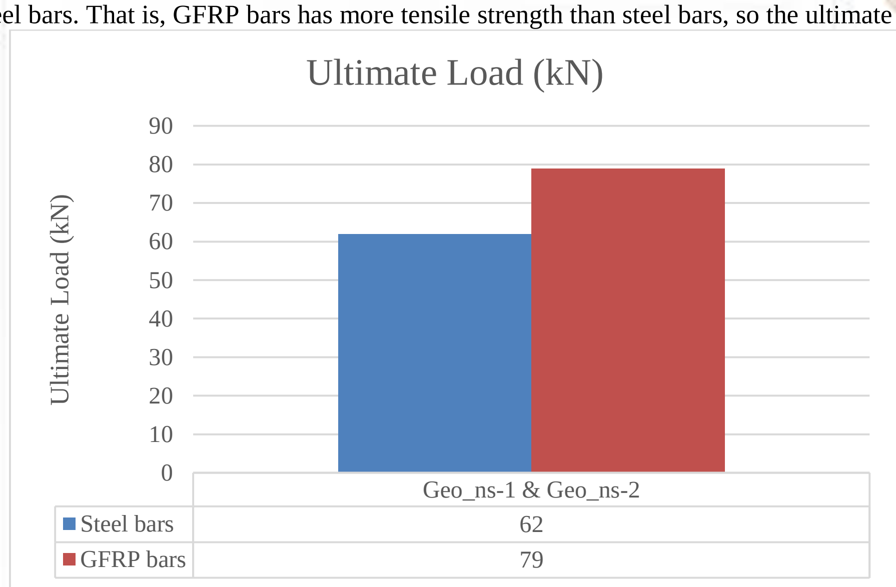

Figure 3. Bar graph representing the ultimate load of beams.

1.2. Ultimate Mid-span Deflection

[Figure 4] represents, the ultimate mid-span deflection of GPC beams. It is noticed that, Geo_ns-1,2 beams have same mid-span deflection of 1.2mm. By using GFRP and steel bars in GPC beam have same ultimate mid-span deflection.

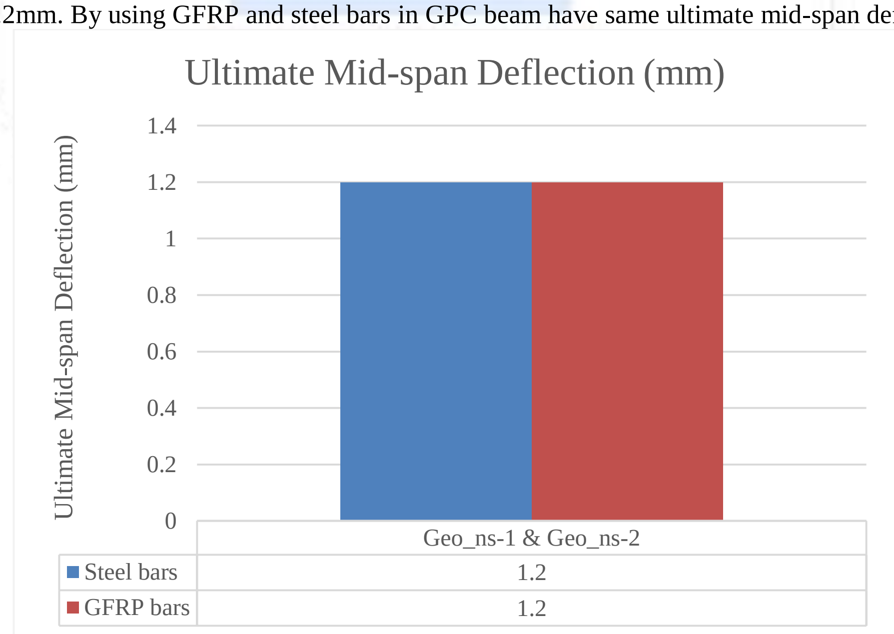

Figure 4. Bar graph representing the ultimate mid-span deflection of beams.

2. Analytical results

2.1. Ultimate load

The ultimate load-carrying capacity of all GPC beams are illustrated in [Figure 5]. It can be identified that Geo_ns-2 beams have maximum load of 70kN whereas Ge_ns-1 beam have maximum load of 55kN. Geo_ns-2 beam have more maximum load-carrying capacity than Geo_ns-1 beam. That is, GFRP bars has greater tensile strength than steel bars, so the ultimate load is increased.

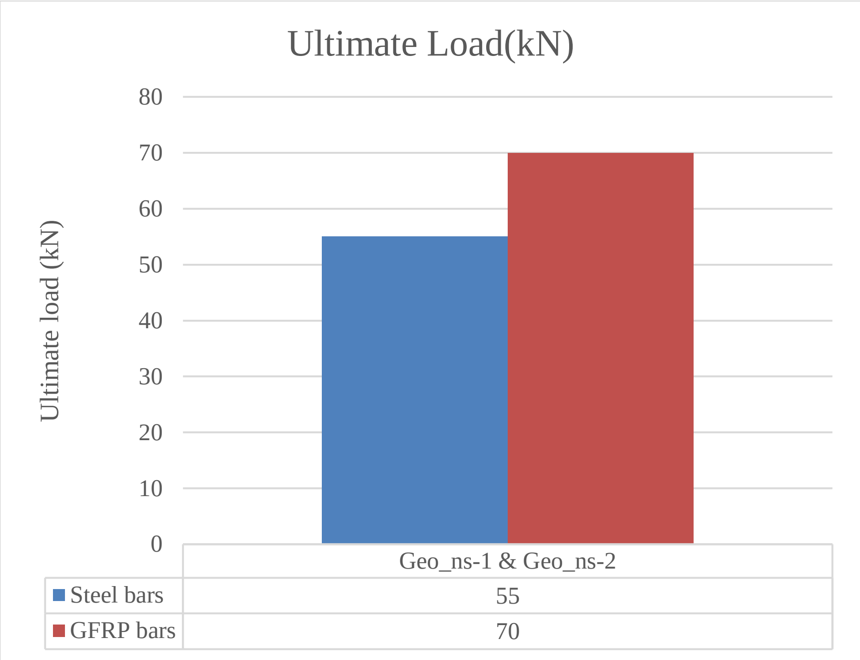

Figure 5. Bar graph representing the ultimate load of beams.

2.2. Ultimate Mid-span Deflection

[Figure 6] represents the ultimate mid-span deflection of GPC beams. It is found that, Geo_ns-2 beam have mid-span deflection of 1.05mm whereas Geo_ns-1 beam have mid-span deflection of 1.2mm. By using GFRP bars in GPC beam have decreased mid-span deflection when compared to GPC beam with steel bars. That is, GFRP bars has greater tensile strength than steel bars, so the ultimate mid-span deflection is reduced.

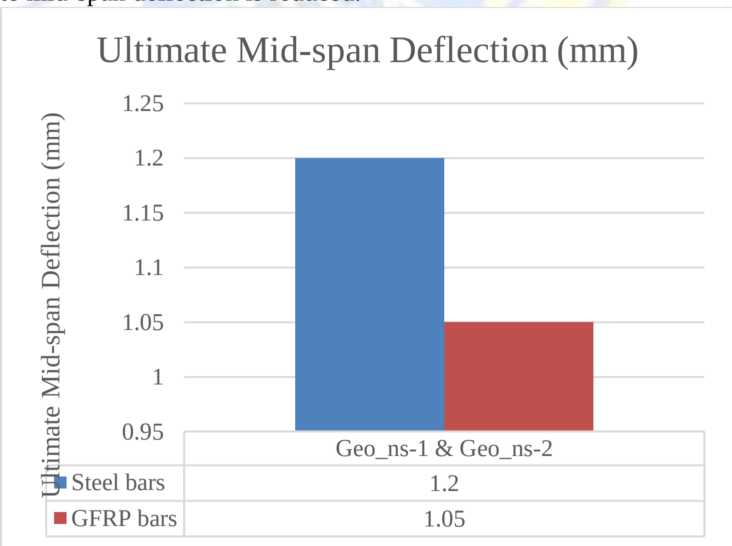

Figure 6. Bar graph representing ultimate mid-span deflection of beams.

3. Comparison of experimental and analytical results

The current study is designed for both analytical and experimental purposes. [Table 4] compare the results obtained through experimental and analytical methods with respect to Ultimate Load and Ultimate mid-span deflection and also provides percentage of variation in the ultimate load and ultimate midspan deflection.

Table 4. Percentage of variation between experimental (Exp) and analytical (FEA) results.

Specimen ID	Ultimate Load (kN) P_{ult}		Ultimate Mid-span Deflection (mm) Δ_{ult}		Comparison of P_{ult} (%) $\frac{Exp - FEA}{\left[\frac{Exp + FEA}{2}\right]} x100$	Comparison of Δ_{ult} (%) $\frac{Exp - FEA}{\left[\frac{Exp + FEA}{2}\right]} x100$
	Exp.	**FEA**	**Exp.**	**FEA**		
Geo_ns-1	62	55	1.2	1	11.9	15.3
Geo_ns-2	79	70	1.2	1.05	12	13.3

The percentage difference in ultimate load and mid-span deflection between experimental and analytical data is tabulated in [Table 4]. Ultimate load is varying between 11.9-12% and ultimate mid-span deflection is varying between 13.3-15.3%.

V. CONCLUSIONS

In the present work, experimental and analytical work is carried out for all the beams. For experimental work, four-point static loading technique was considered and analysis was carried out by using ANSYS 2022 software. The comparison is made for experimental and analytical results. From the outcomes of the experimental work, by using GFRP bars in GPC beam the ultimate load carrying capacity was found to be increased by 24.11% than GPC with steel bars. As per experimental investigation, it is noticed that, GPC beam with GFRP and steel bars have same ultimate mid-span deflection. The experimental and analytical results were showing the same trend for both ultimate load and ultimate mid-span deflection. Ultimate load is varying between 11.9-12% and ultimate mid-span deflection is varying between 13.3-15.3%.

VI. REFERENCES

[1] Abdallah, M., Al Mahmoud, F., Khalil, N., & Khelil, A. (2023). Effect of the strengthening patterns on the flexural performance of RC continuous beams using FRP reinforcements. *Engineering Structures*, *280*, 115657. Elsevier. Available from: https://doi.org/10.1016/j.engstruct.2023.115657

[2] Lu, C., Cai, Q., Xu, K., Sha, X., & Yan, Y. (2022, September). Comparison of flexural behaviors between plain and steel-fiber-reinforced concrete beams with hybrid GFRP and steel bars. In *Structures* (Vol. 43, pp. 1-11). Elsevier. Available from: https://doi.org/10.1016/j.istruc.2022.06.037

[3] Junaid, M. T., Karzad, A. S., Elbana, A., & Altoubat, S. (2022, January). Experimental study on shear response of GFRP reinforced concrete beams strengthened with externally bonded CFRP sheets. In *Structures* (Vol. 35, pp. 1295-1307). Elsevier. Available from: https://doi.org/10.1016/j.istruc.2021.10.089

[4] Liu, S., Wang, X., Ali, Y. M., Su, C., & Wu, Z. (2022). Flexural behavior and design of under-reinforced concrete beams with BFRP and steel bars. *Engineering Structures*, *263*, 114386. Elsevier. Available from: https://doi.org/10.1016/j.engstruct.2022.114386

[5] El-Sayed, T. A., & Algash, Y. A. (2021). Flexural behavior of ultra-high performance geopolymer RC beams reinforced with GFRP bars. *Case Studies in Construction Materials*, *15*, e00604. Elsevier. Available from: https://doi.org/10.1016/j.cscm.2021.e00604

[6] Huang, Z., Chen, W., Hao, H., Chen, Z., Pham, T. M., Tran, T. T., & Elchalakani, M. (2021). Shear behaviour of ambient cured geopolymer concrete beams reinforced with BFRP bars under static and impact loads. *Engineering Structures*, *231*, 111730. Elsevier. Available from: https://doi.org/10.1016/j.engstruct.2020.111730

[7] Aravind, N., Nagajothi, S., & Elavenil, S. (2021). Machine learning model for predicting the crack detection and pattern recognition of geopolymer concrete beams. *Construction and Building Materials*, *297*, 123785. Elsevier. Available from: https://doi.org/10.1016/j.conbuildmat.2021.123785

[8] Rashid, K., Li, X., Xie, Y., Deng, J., & Zhang, F. (2020). Cracking behavior of geopolymer concrete beams reinforced with steel and fiber reinforced polymer bars under flexural load. *Composites Part B: Engineering*, *186*, 107777. Available from: https://doi.org/10.1016/j.compositesb.2020.107777

[9] Barris, C., Sala, P., Gómez, J., & Torres, L. (2020). Flexural behaviour of FRP reinforced concrete beams strengthened with NSM CFRP strips. *Composite Structures*, *241*, 112059. Elsevier. Available from: https://doi.org/10.1016/j.compstruct.2020.112059

[10] Junaid, M. T., Elbana, A., & Altoubat, S. (2020, April). Flexural response of geopolymer and fiber reinforced geopolymer concrete beams reinforced with GFRP bars and strengthened using CFRP sheets. In *Structures* (Vol. 24, pp. 666-677). Elsevier. Available from: https://doi.org/10.1016/j.istruc.2020.02.003